Limits of Strong Field Rescattering in the Relativistic Regime

M. Klaiber, K. Z. Hatsagortsyan, J. Wu, S. S. Luo, P. Grugan, and B. C. Walker

Phys. Rev. Lett. **118**, 093001 — Published 27 February 2017

DOI: 10.1103/PhysRevLett.118.093001

Limits of strong field rescattering in the relativistic regime

M. Klaiber,[1] K. Z. Hatsagortsyan,[1,*] J. Wu,[2] S.S. Luo,[3] P. Grugan,[3] and B. C. Walker[3,†]

[1] *Max-Planck-Institut für Kernphysik, Saupfercheckweg 1, 69117 Heidelberg, Germany*
[2] *State Key Laboratory of Precision Spectroscopy, East China Normal University, Shanghai 200062, China*
[3] *Department of Physics and Astronomy, University of Delaware, Newark, Delaware 19716, USA*

(Dated: January 19, 2017)

Recollision for a laser driven atomic system is investigated in the relativistic regime via a strong field quantum description and Monte-Carlo semi-classical approach. We find the relativistic recollision energy cutoff is independent of the ponderomotive potential U_p, in contrast to the well-known $3.2U_p$-scaling. The relativistic recollision energy cutoff is determined by the ionization potential of the atomic system and achievable with non-negligible recollision flux before entering a "rescattering free" interaction. The ultimate energy cutoff is limited by the available intensities of short wavelength lasers and cannot exceed a few thousand Hartree, setting a boundary for recollision based attosecond physics.

PACS numbers: 32.80.Rm,34.80.Dp,78.47.J-

Rescattering [1, 2] between a photoelectron and parent ion is an essential physical process underpinning twenty years of advances in coherent x-ray radiation generation [3, 4], insight into multielectron dynamics [5, 6], and the launch of attosecond science [7, 8]. The highest energy for a laser driven rescattering collision between a photoelectron and the ionizing parent ion is described by a '$3.2U_p$' rule [9], where $U_p = e^2E_0^2/(4m\omega^2)$ is the kinetic quiver energy, or ponderomotive energy, of a free electron charge e mass m in an oscillating electric field amplitude E_0 frequency ω. Elastic scattering of the photoelectron when it 're'-encounters the parent ion at this energy is responsible for the high energy plateau in the above-threshold ionization (ATI) [10] and has been used to image electron wave functions of molecules [11, 12]. Inelastic scattering, including multielectron nonsequential (e,ne) ionization (NSI) [13], is a mechanism to further excite the parent ion and can photoinitiate inner-shell excitation (ISE) processes [14]. Recombination with the parent ion during recollision gives rise to coherent high-order harmonic generation (HHG) and can produce soft x-ray, attosecond radiation [15]. As the strong field science frontier expands to higher intensities, relativistic effects enter into play. For atomic systems a Lorentz deflection parameter [16] was proposed as a way to gauge their impact,

$$\Gamma_R = \frac{\sqrt{2I_p mc^2}a_0^3}{16\hbar\omega}, \qquad (1)$$

where $a_0 = eE_0/(mc\omega)$ is the Lorentz invariant field parameter [17]. For $\Gamma_R > 1$ the Lorentz force due to the laser magnetic field can deflect the photoelectron position by more than the electron wave packet extent in space at the recollision moment, significantly reducing the recollision probability and related phenomena [18–24]. The attenuation is especially large at higher recollision energies, which effectively constrains the HHG cutoff in the relativistic regime [23–26]. Changes to HHG in the relativistic regime have been recognized theoretically for more than ten years;

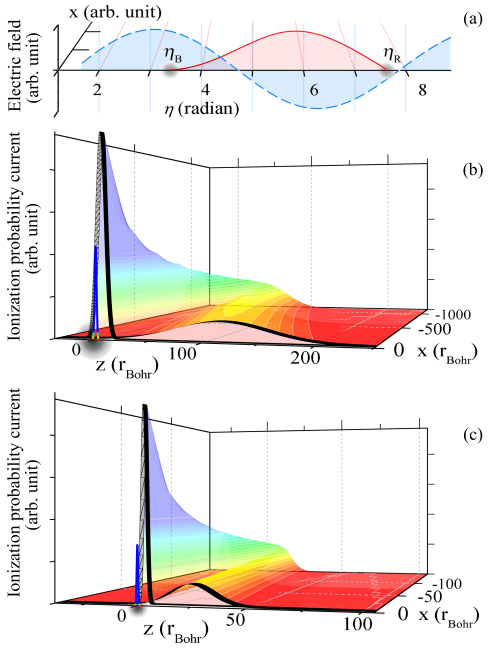

FIG. 1. (color online) (a) Trajectory (solid-red) for photoelectron born (η_B) and returning to the parent ion (η_R) in an oscillating electric field (dashed-blue) for the peak "$3.2U_p$" recollision. Corresponding ionization probability current $\mathbf{j}(\mathbf{r}, \eta_B)$ for Ar^{4+} ionization at 4.6×10^{15} W/cm^2, 2400 nm (b); and Ar^{9+}, 1.6×10^{18} W/cm^2, 200 nm (c). In (b,c) the initial localized $\mathbf{j}(0, \eta_B)$ magnitude is divided by ten.

shaped or counter propagating laser pulses and additional fields have been proposed to counteract this Lorentz drift and realize HHG in the relativistic domain [25–38]. For ultrahigh intensities ($\Gamma_R \gg 1$), the Lorentz deflection is very large and there is no observed interaction between the photoelectron and parent ion [39, 40].

What has remained elusive is a general quantitative de-

scription for the relativistic rescattering cutoff and yield at the limits of rescattering. For example, how the recollision energy and the recollision flux scale with laser or atomic parameters at large Γ_R and what ultimate recollision energy is achievable. The answers to these questions are vital to set the boundary for attosecond physics based on the recollision concept. In particular, for the generation of hard x-ray attosecond radiation [41] and laser induced electron diffraction imaging used to investigate dynamics with sub-angstrom, attosecond precision [42, 43].

In this letter we investigate the rescattering process in the relativistic regime and describe quantitatively its limits in terms of recollision flux and recollision energy. The recollision photoelectron flux is calculated quantum mechanically using the relativistic Coulomb-corrected strong field approximation (RCCSFA) and semi-classically with a Monte-Carlo trajectory ensemble (SCMC) method. For a broad range of species in different laser fields, we find the rescattering flux can be non-negligible in the relativistic regime, $\Gamma_R > 1$, yielding recollision cutoff energies with a scaling different from the well-known $3.2U_p$-rule. The scaling laws for the ultimate energy cutoff and corresponding flux are derived via intuitive estimations. We show the ultimate energy cutoff at $\Gamma_R \gg 1$ is practically limited by the available intensities of the short wavelength lasers and cannot exceed a few thousand Hartree.

We begin by discussing the rescattering photoelectron before ensuing elastic, inelastic and recombination processes. We study intensities from 10^{13} W/cm^2 to 10^{21} W/cm^2 with wavelengths from 80 nm to 8 μm. Across this span we use highly charged ion (HCI) states for argon (Ar^{Z+}, $1 \le Z \le 17$) in external fields with amplitudes $E_0 \le 0.95 E_{\rm OBI}$, where $E_{\rm OBI} = I_p^2/(4e^3Z)$ is the classical over-barrier-ionization (OBI) field [44]. The tunneling regime of ionization is considered since $\hbar\omega \ll I_p$ and the Keldysh adiabaticity $\gamma = \omega\sqrt{2mI_p}/(eE_0)$ is much less than one [45]. The calculated tunneling ionization probability per laser cycle W_0 is kept below 50%. Depletion of the tunneling ion ground state in the rising edge of the laser pulse is not substantial; the results are comparable to experiments near saturation with few cycle pulses. Changing to other atomic species does not alter our findings.

Once in the continuum a tunneling photoelectron current density $\mathbf{j}$ is used to describe the electron, including the rescattering portion $\mathbf{j}_R$ that revisits the parent ion. The rate for a rescattering process ($\frac{dw_R}{dt}$) can be estimated via the photoelectron rescattering current density and the cross-section of the process (σ_R): $\frac{dw_R}{dt} = \sigma_R j_R$. A more relevant physical quantity in rescattering is the probability per unit energy during one laser cycle $\frac{dw_R}{d\varepsilon} = \sigma_R \frac{dF_R}{d\varepsilon}$, which is determined by the flux per unit energy

$$\frac{dF_R}{d\varepsilon} = j_R \frac{dt}{d\varepsilon}. \tag{2}$$

In our quantum mechanical treatment the rescattering flux is calculated via RCCSFA based on the Dirac equation [47–49]. The wave function of the electron ionized from a hydrogen-like atomic bound state $|\phi_0(\eta)\rangle$ in a strong laser field $\mathbf{E}(\eta) = -\mathbf{A}'(\eta)$, with the vector-potential $\mathbf{A}(\eta) = (E_0/\omega)\sin(\eta)\hat{x}$, and the laser phase $\eta = \omega(t - z/c)$, is given by [49]:

$$\psi(\mathbf{r},\eta) = -\int d^3\mathbf{q} \int \frac{d\eta'}{\omega} \langle \mathbf{r}|\mathbf{q}(\eta)\rangle \langle \mathbf{q}(\eta')|\mathbf{r}\cdot\mathbf{E}(\eta')Q|\phi_0(\eta')\rangle \times \exp[-iS(\mathbf{q},\eta,\eta')], \tag{3}$$

where $|\mathbf{q}(\eta)\rangle$ is the relativistic momentum state of

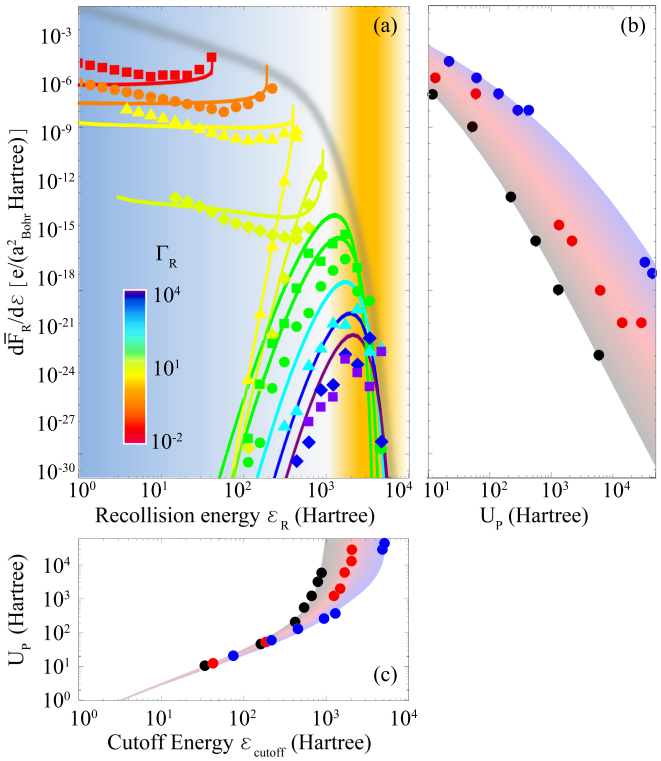

FIG. 2. (color online) Normalized differential rescattering flux (a) via RCCSFA (line) and SCMC (symbol) for the laser wavelength $\lambda = 800$ nm. Line color scales with Γ_R: Ar^{5+} at 5.8×10^{15} W/cm^2 ($\Gamma_R = 0.06$, square); Ar^{7+} 2.7×10^{16} W/cm^2 ($\Gamma_R = 0.7$, circle); Ar^{8+} 5.6×10^{16} W/cm^2 ($\Gamma_R = 3.8$, triangle); Ar^{8+} 1.3×10^{17} W/cm^2 ($\Gamma_R = 13$, diamond); Ar^{8+} at 6×10^{17} W/cm^2 ($\Gamma_R = 140$, square); Ar^{9+} at 1×10^{18} W/cm^2 ($\Gamma_R = 320$, circle); Ar^{11+} at 2.8×10^{18} W/cm^2 ($\Gamma_R = 1{,}700$, triangle); Ar^{13+} at 6.3×10^{18} W/cm^2 ($\Gamma_R = 6{,}100$, diamond); Ar^{14+} at 1.3×10^{19} W/cm^2 ($\Gamma_R = 20{,}000$, square). In (a) the change from traditional rescattering (blue) to the relativistic cutoff region (orange) is highlighted in the background and a shadow line gives the typical highest possible $d\bar{F}_R/d\varepsilon$ at optical frequencies. For clarity, long and short contributions to $d\bar{F}_R/d\varepsilon$ are summed in the nonrelativistic limit $\Gamma_R < 1$. For RCCSFA with argon HCI [46], $d\bar{F}_R/d\varepsilon$ at cutoff as a function of U_p is shown in (b) and the relationship between U_p and the recollision cutoff energy is given (c) for laser wavelengths 80 nm (blue), 800 nm (red), and 8000 nm (black) with shading to aid the eye.

the photoelectron before recollision, $Q = (-4I_p/(\mathbf{r}\cdot\mathbf{E}(\eta')))^{Z/(2I_p)^{1/2}}$ is the Coulomb correction factor, $S(\mathbf{q},\eta,\eta') = \int_{\eta'}^{\eta} d\eta''[\varepsilon_{\mathbf{q}}(\eta'') - mc^2 + I_p]/\omega$, with the electron energy and momentum in the laser field $\varepsilon_{\mathbf{q}}(\eta) = \varepsilon_{\mathbf{q}} + c^2[\mathbf{q}\cdot\mathbf{A}(\eta) + \mathbf{A}(\eta)^2/(2\Lambda)]$, $\mathbf{q}(\eta) = \mathbf{q} + \mathbf{A}(\eta) + c^2[\mathbf{q}\cdot\mathbf{A}(\eta) + \mathbf{A}(\eta)^2/(2\Lambda)]$, respectively, $\varepsilon_{\mathbf{q}} = c^2\sqrt{m^2c^2 + \mathbf{q}^2}$, and $\Lambda = \varepsilon_{\mathbf{q}}(\eta) - c\hat{z}\cdot\mathbf{q}(\eta)$ is the integral of motion in the plane laser field; unit vectors $\hat{x}$,$\hat{y}$, and $\hat{z}$ point in the laser electric, magnetic field, and propagation directions, respectively.

The quantum wave function allows us to obtain the rescattering probability current density at the atomic core, by inserting the $\mathbf{r} = 0$ condition into the current density expression ($\mathbf{j}_R(0,\eta_R) = \mathbf{q}(\eta_R)|\psi(0,\eta_R)|^2/(2\pi)^3$) and calculating the differential flux from Eq. (2). The four-dimensional integral for $\mathbf{j}_R(0,\eta_R)$ is solved with the saddle point method, which also yields for each recollision η_R an initial 'birth' phase η_B (Fig. 1). The RCCSFA accounts for the Coulomb field effects in the tunneling step of ionization, yielding a tunneling rate that coincides with the relativistic extension of the Perelomov-Popov-Terent'ev (PPT) theory [50–53]. For our purposes and to a high degree of accuracy, PPT is the same as the nonrelativistic Ammosov, Delone, and Krainov (ADK) tunneling rate [54] shown to describe ionization up to intensities of 10^{19} W/cm^2 [55].

Our semi-classical SCMC calculation follows the quantum calculation. Briefly, for each time in the optical cycle the ADK ionization rate is used to quantify the initial current density $\mathbf{j}(\mathbf{r},\eta_B)$ at the tunneling barrier, which is then represented by an ensemble of trajectories given an initial spatial width (and corresponding momentum uncertainty) perpendicular to the electric field. The ensemble current density propagates relativistically in the fields of the laser and the atomic core, providing the SCMC $\mathbf{j}_R(0,\eta_R)$ recollision flux and $\frac{\partial F_R}{\partial\varepsilon}$ [56]. We note that in both quantum and semi-classical treatments, contributions from multiple returns are not considered.

In Fig. 2 the differential rescattering flux normalized to W_0, (i.e. $\frac{d\overline{F}_R}{d\varepsilon} \equiv \frac{1}{W_0}\frac{dF_R}{d\varepsilon}$), is shown for argon HCI. Nonrelativistic rescattering flux ($\Gamma_R \lesssim 1$) show the well-known characteristic plateau extending up to $3.2U_p$, where the flux peaks and then drops to zero [1]. As rescattering moves into the relativistic domain ($\Gamma_R \gtrsim 1$), a change occurs in the form of the flux distribution from a plateau to a 'looping bow'. The peak of the loop is the maximum return energy, approximately $3.2U_p$, and the two ends of the bow are the energetically degenerate collisions in the field commonly described as long and short trajectories. As Γ_R increases, the normally dominant long trajectory contribution to $d\overline{F}_R/d\varepsilon$ is suppressed by the extended time in the Lorentz force.

Proceeding to the ultrarelativistic recollision regime ($\Gamma_R \sim 100$) long trajectories are deflected by many times the spatial width of $\mathbf{j}_R(0,\eta_R)$. Only a diminishing $d\overline{F}_R/d\varepsilon$ 'peak' remains from a narrow range of short trajectories able to return to the parent ion (similar features are shown in HHG spectra [23–25]). A characteristic feature of relativistic recollision is, regardless of increasing Γ_R or U_p, the ultimate cutoff energy does not change. The recollision flux has been calculated for a broad range of wavelengths and HCIs [46]. Our conclusion and the extreme limits of possible strong field interactions (far ultraviolet, optical, far infrared) are presented in Fig. 2(b,c). We see in Fig. 2(b) that, while decreasing with the growth of Γ_R, the flux is not negligible at large Γ_R. In Fig. 2(a,c) we show the cutoff energy scaling begins to deviate from the $3.2U_p$ rule beyond ponderomotive energies of a few hundred Hartree ($\Gamma_R > 1$), with the cutoff ε_{cutoff} saturating and reaching an ultimate limit of a few thousand Hartree even as U_p exceeds 10^4 Hartree ($\Gamma_R > 100$).

In Fig. 1 we can inspect the ionization probability current $\mathbf{j}$ corresponding to a peak rescattering energy. Two species are shown in juxtaposition; Ar^{4+} at 4.6×10^{15} W/cm^2, 2400 nm, and Ar^{9+} at 1.6×10^{18} W/cm^2, 200 nm. On first inspection these two cases seem very different by laser intensity, wavelength, and ionization potentials. Fig. 1 follows the ionization current $\mathbf{j}$ from birth (η_B) at the parent ion (origin) to recollision (η_R). Initially, $\mathbf{j}(0,\eta_B)$ is highly localized at the parent ion with an initial spatial width χ_i of the order of the Bohr radius, $\chi_i \sim r_{Bohr}$. After moving only a few percent of the single cycle displacement from the parent ion (black outline at x = -44 r_{Bohr} and -5 r_{Bohr} in Fig. 1(b,c), respectively), the spatial width of $\mathbf{j}$ is overwhelmed by spreading from momentum uncertainty. The continuum electron for Ar^{4+} extends 1200 Bohr in x and is deflected by > 100 Bohr in z, while Ar^{9+} extends to 100 Bohr and is deflected by $\sim$ 25 Bohr. Nevertheless, near the recollision point there is a clearly observable consistency in the deflection with respect to the electron wave packet size.

To better understand rescattering, we estimate the rescattering current density using the rescattering velocity v_R, the electron wave packet spatial extent at recollision along $\hat{x},\hat{y},\hat{z}$-directions ($\chi_{x,y,z}$), and the Lorentz deflection parameter Γ_R:

$$j_R \sim \frac{W_0 v_R}{\chi_x\chi_y\chi_z}\exp(-\Gamma_R), \tag{4}$$

where the exponential factor stems from the fact rescattering in the relativistic regime is attained by the electron tunneled out from the atom with an initial momentum compensating the drift momentum in the laser propagation direction $p_z \sim -U_p/c$, the probability of the latter being $\exp\left(-p_z^2/\Delta p_z^2\right) = \exp\left(-\Gamma_R\right)$, with $\Delta p_z = (eE\hbar)^{1/2}/(2I_p/m)^{1/4}$ [57]. We tested our estimation in the nonrelativistic regime [46] and focus our discussion here on dynamics in the relativistic regime $\Gamma_R \gg 1$. As the Lorentz force increases, photoionization must be 'launched' closer to the laser field zero-crossing at a field $E(\eta_B) \approx E_0\eta_B$ to avoid being de-

flected. In this cutoff region we estimate the laser phase η_B for the most probable ionization of the short rescattering trajectories, using the scaling of the tunneling ionization probability: $\propto \exp\left[-2E_a/(3E_0\eta_B) - \Gamma_R\eta_B^3\right]$, where the rescattering from fields near zero-crossing rather than the peak field is incorporated by replacing E_0 with $E(\eta_B)$ in the Γ_R expression of Eq. (1) and we have used the atomic field $E_a \equiv (2I_p)^{3/2}\sqrt{m}/e\hbar$. From the exponent above, the short rescattering trajectories within the cutoff are most probably launched at the laser phase $\eta_{cutoff} \approx (1.37/a_0)(2I_p/mc^2))^{1/4}$ near the laser zero-crossing and correspond to a recollision energy of $\varepsilon_{cutoff} \approx 3.2mc^2a_0^2\eta_{cutoff}^2/4$, which reads

$$\varepsilon_{cutoff} \approx 1.5\sqrt{2I_pmc^2}. \tag{5}$$

Thus, the well-known 3.2 U_p rule for the recollision cutoff energy is replaced in the relativistic regime $\Gamma_R \gg 1$ by Eq. (5), which indicates a cutoff for the corresponding peak of the bell-shape flux distribution that tends to the constant value in the relativistic domain, see Fig. 2(c) [46].

A reasonable prediction for the relativistic rescattering flux at $\Gamma_R \gg 1$ (Fig. 2(b)) can be obtained in the cutoff region from Eq. (4), with $\eta_B = \eta_{cutoff}$, and the electron wave packet extensions $\chi_x \sim \lambda a_0$, $\chi_y \sim \lambda a_0^2$, and $\chi_z = \Delta p_z/(m\omega)$:

$$\frac{d\overline{F}_R(\varepsilon_R)}{d\varepsilon} \sim \frac{\sqrt{2\varepsilon_R/m}\, e^{-\Gamma_R\eta_{cutoff}^3}}{\chi_x\chi_y\chi_z\omega\varepsilon_R} \sim \frac{e^{-\frac{1}{16}\frac{mc^2}{\hbar\omega}\left(\frac{2I_p}{mc^2}\right)^{5/4}}}{\lambda^2 a_0^3\sqrt{a_0\hbar\omega mc^2}} \tag{6}$$

The region of the non-negligible flux (up to $\Gamma_R \sim 100$ [46]) can be estimated from the exponential factor of Eq. (6): $\hbar\omega \sim (mc^2/16)(2I_p/mc^2)^{5/4}$. To extend the relativistic cutoff a large I_p is required, which calls for a large laser intensity as well as a short laser wavelength. For instance with infrared lasers ($\lambda = 800$ nm, $I \sim 10^{17}$ W/cm^2) one can achieve an ultimate recollision energy of $\varepsilon_R \sim 1000$ Hartree, while with ultraviolet lasers ($\lambda = 200$ nm, $I \sim 10^{19}$ W/cm^2) $\varepsilon_R \sim 2000$ Hartree.

Considering the laser field as an 'optical scale' laser accelerator, the ultimate cutoff represents the acceleration energy where the electron from an atom (atomic radius $r_a \sim \hbar/\sqrt{2I_pm}$) will be deflected by its width and miss the parent ion at rescattering. Returning to the Lorentz deflection parameter expressed as $\Gamma_R \approx U_p^2\chi_i^2/(\hbar^2c^2)$ and setting $\Gamma_R = 1$, one can see for any system with an initial extent $\chi_i = r_a$ an electron accelerated in a radiation field will have an ultimate cutoff of $U_p = c\sqrt{2I_pm}$, i.e., a 3.2 U_p rescattering energy limit of 10^3 Hartree.

The significance of an ultimate cutoff is clear as rescattering is the mechanism for high energy ATI, NSI, HHG, and ISE. We briefly here show the impact on ATI. The angle resolved differential ATI rate is calculated quantum

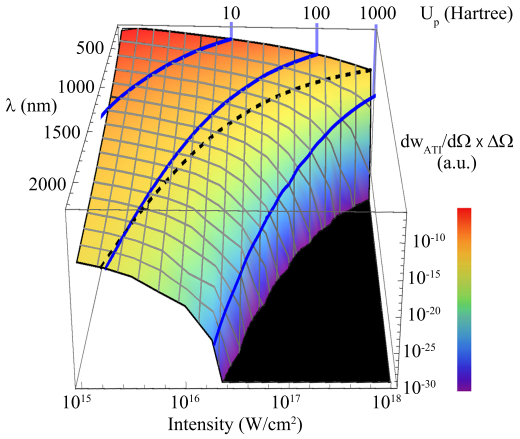

FIG. 3. (color online) ATI as a function of laser intensity and wavelength for photoelectron energies near $10U_p$. Blue lines indicate $U_p = 10, 100, 1000$ a.u. The dashed line corresponds to $\Gamma_R = 1$. The color scale for ATI spans from 10^{-30} to 10^{-6} a.u.

mechanically using RCCSFA: $\frac{dw_{\rm ATI}}{d\Omega} = \frac{\omega^2 p\varepsilon_{\mathbf{p}}}{c^2}|M_{\mathbf{p}}|^2$, with

$$M_{\mathbf{p}} = -\int d\eta \int d\eta' \int d^3\mathbf{q}\langle\mathbf{p}(\eta)|V|\mathbf{q}(\eta)\rangle\langle\mathbf{q}(\eta')|\mathbf{r}\cdot\mathbf{E}(\eta')Q|\phi_0(\eta')\rangle \times \exp[-iS(\mathbf{p},\infty,\eta)] - iS(\mathbf{q},\eta,\eta')] \tag{7}$$

where $\mathbf{p}(\eta) = \mathbf{p}+\mathbf{A}(\eta)+\mathbf{T}(\eta,\mathbf{p})$, $\mathbf{q}(\eta) = \mathbf{q}+\mathbf{A}(\eta)+\mathbf{T}(\eta,\mathbf{q})$ are the relativistic kinetic momentum after the recollision and during excursion, respectively, the drift momentum $\mathbf{T}(\eta,\mathbf{p}) = \hat{z}[\mathbf{p}\cdot\mathbf{A}(\eta) + \mathbf{A}^2(\eta)/2]/c$, and $V(r)$ is the Coulomb-potential of the atomic core [58]. The findings presented here are not changed for CTMC calculations with more accurate potentials using numerical Dirac−Fock electron densities [59].

The energy resolved ionization is evaluated by integrating the outgoing photoelectron over an effective solid angle of $\Delta\Omega = \pi/8$. In Fig. 3, high-order ATI as function of the laser intensity and wavelength is shown plotted for electrons with a final energy (at the detector) of $10U_p \pm U_p/2$. We see the probability of elastic scattering with recollision energies beyond the ultimate cutoff of ~ 1000 a.u. is precipitously suppressed with the drop in ATI after one crosses the $\Gamma_R = 1$ threshold. For the same recollision energy the probability of elastic scattering is larger when using short wavelength lasers, consistent with a $\lambda^{-4/3}$ scaling that can be obtained from Eq. (4). Elastic scattering with a recollision energy of 30 Hartree ($U_p = 10$) can be achieved with $\lambda = 1700$ nm (at 10^{15} W/cm^2) as well as with $\lambda = 200$ nm (at 4×10^{16} W/cm^2); however, in the shorter wavelength case the ATI rate is larger by four orders of magnitude.

Our calculations so far have involved single electron dynamics. Clearly, as rescattering energies increase many electrons are excited [60, 61]. For a recollision of several hundred Hartree, the new possibility of exciting all

bound states in high Z atoms becomes possible. Further clarification of multielectron physics [62] will be required to better understand such highly excited species. We have extended our analysis to consider ionization at any phase η_B, rather than limited by tunneling. These results indicate that electrons ionized at any time during the laser cycle, e.g. by inner shell thermalization, will still be limited by the ultimate cutoff.

In conclusion, we have calculated the ultimate limit of rescattering in laser fields. The presented relativistic quantum and semi-classical calculations show for a broad range of species in different laser fields that rescattering continues to be important in the relativistic regime ($\Gamma_R \geq 1$) and has an ultimate energy cutoff for $\Gamma_R \gg 1$. Scaling laws for the ultimate energy cutoff and flux are derived. The cutoff energy changes from a strong field $3.2U_p$-rule to a relativistic limit of $\varepsilon_{cutoff} \approx 1.5\sqrt{2I_p mc^2}$, beyond which the recollision process in a given species will cease to contribute to ATI, HHG, and ISE. We show the ultimate energy cutoff and highest rescattering flux is best realized by intense, short wavelength lasers and cannot exceed a few thousand Hartree, indicating hard x-rays via recollision induced HHG [37, 63] can be extended to photon energies of 60 keV.

MK and KZH acknowledge fruitful discussions with C. H. Keitel. This material is based upon work supported by the National Science Foundation under Grant No. 1607321 and No. 1307042.

* k.hatsagortsyan@mpi-k.de
† bcwalker@udel.edu

[1] P. B. Corkum, Phys. Rev. Lett. **71**, 1994 (1993).
[2] W. Becker, F. Grasbon, R. Kopold, D. Milošević, G. G. Paulus, and H. Walther, Adv. Atom. Mol. Opt. Phys. **48**, 35 (2002).
[3] M. Ferray, A. L'Huillier, X. Li, L. Lompre, G. Mainfray, and C. Manus, J. Phys. B **21**, L31 (1988).
[4] M. Chini, K. Zhao, and Z. Chang, Nat. Photon. **8**, 178 (2014).
[5] B. Walker, B. Sheehy, L. Dimauro, P. Agostini, K. Schafer, and K. Kulander, Phys. Rev. Lett. **73**, 1227 (1994).
[6] W. Becker, X. Liu, P. J. Ho, and J. H. Eberly, Rev. Mod. Phys. **84**, 1011 (2012).
[7] P. Paul, E. Toma, P. Breger, G. Mullot, F. Auge, P. Balcou, H. Muller, and P. Agostini, Science (N.Y.) **292**, 1689 (2001).
[8] F. Krausz and M. Ivanov, Rev. Mod. Phys. **81**, 163 (2009).
[9] K. Schafer, B. Yang, L. Dimauro, and K. Kulander, Phys. Rev. Lett. **70**, 1599 (1993).
[10] B. Yang, K. J. Schafer, B. Walker, K. C. Kulander, P. Agostini, and L. F. DiMauro, Phys. Rev. Lett. **71**, 3770 (1993).
[11] J. Itatani, J. Levesque, D. Zeidler, H. Niikura, H. Pépin, J. C. Kieffer, P. B. Corkum, and D. M. Villeneuve, Nature **432**, 867 (2004).
[12] Y. Huismans, A. Rouzée, A. Gijsbertsen, J. H. Jungmann, A. S. Smolkowska, P. S. W. M. Logman, F. Lépine, C. Cauchy, S. Zamith, T. Marchenko, J. M. Bakker, G. Berden, B. Redlich, A. F. G. van der Meer, H. G. Muller, W. Vermin, K. J. Schafer, M. Spanner, M. Y. Ivanov, O. Smirnova, D. Bauer, S. V. Popruzhenko, and M. J. J. Vrakking, Science (N.Y.) **331**, 61 (2011).
[13] R. Moshammer, B. Feuerstein, W. Schmitt, A. Dorn, C. Schroter, J. Ullrich, H. Rottke, C. Trump, M. Wittmann, G. Korn, K. Hoffmann, and W. Sandner, Phys. Rev. Lett. **84**, 447 (2000).
[14] Y. Deng, Z. Zeng, Z. Jia, P. Komm, Y. Zheng, X. Ge, R. Li, and G. Marcus, Phys. Rev. Lett. **116**, 073901 (2016).
[15] D. Popmintchev, C. Hernández-García, F. Dollar, C. Mancuso, J. A. Perez-Hernandez, M.-C. Chen, A. Hankla, X. Gao, B. Shim, A. L. Gaeta, M. Tarazkar, D. A. Romanov, R. J. Levis, J. A. Gaffney, M. Foord, S. B. Libby, A. Jaron-Becker, A. Becker, L. Plaja, M. M. Murnane, H. C. Kapteyn, and T. Popmintchev, Science **350**, 1225 (2015).
[16] S. Palaniyappan, I. Ghebregziabher, A. DiChiara, J. MacDonald, and B. C. Walker, Phys. Rev. A **74**, 033403 (2006).
[17] A. Di Piazza, C. Müller, K. Z. Hatsagortsyan, and C. H. Keitel, Rev. Mod. Phys. **84**, 1177 (2012).
[18] C. H. Keitel and P. L. Knight, Phys. Rev. A **51**, 1420 (1995).
[19] M. W. Walser, C. H. Keitel, A. Scrinzi, and T. Brabec, Phys. Rev. Lett. **85**, 5082 (2000).
[20] M. Dammasch, M. Dörr, U. Eichmann, E. Lenz, and W. Sandner, Phys. Rev. A **64**, 061402 (2001).
[21] N. J. Kylstra, R. M. Potvliege, and C. J. Joachain, J. Phys. B **34**, L55 (2001).
[22] J. Prager and C. H. Keitel, J. Phys. B **35**, L167 (2002).
[23] D. B. Milošević, S. Hu, and W. Becker, Phys. Rev. A **63**, 011403(R) (2000).
[24] D. B. Milošević, S. X. Hu, and W. Becker, Laser Phys. **12**, 389 (2002).
[25] C. C. Chirilă, C. J. Joachain, N. J. Kylstra, and R. M. Potvliege, Phys. Rev. Lett. **93**, 243603 (2004).
[26] H. K. Avetissian, A. G. Markossian, and G. F. Mkrtchian, Physics Letters A **375**, 3699 (2011).
[27] C. C. Chirilă, N. J. Kylstra, R. M. Potvliege, and C. J. Joachain, Phys. Rev. A **66**, 063411 (2002).
[28] G. R. Mocken and C. H. Keitel, J. Phys. B **37**, L275 (2004).
[29] N. Milosevic, P. B. Corkum, and T. Brabec, Phys. Rev. Lett. **92**, 013002 (2004).
[30] M. Klaiber, K. Z. Hatsagortsyan, and C. H. Keitel, Phys. Rev. A **74**, 051803 (2006).
[31] Q. Lin, S. Li, and W. Becker, Opt. Lett. **31**, 2163 (2006).
[32] R. Fischer, M. Lein, and C. H. Keitel, Phys. Rev. Lett. **97**, 143901 (2006).
[33] M. Verschl and C. H. Keitel, EPL **77**, 64004 (2007).
[34] M. Klaiber, K. Z. Hatsagortsyan, C. Müller, and C. H. Keitel, Opt. Lett. **33**, 411 (2008).
[35] M. Verschl, Laser Phys. **18**, 598 (2008).
[36] M. C. Kohler, M. Klaiber, K. Z. Hatsagortsyan, and C. H. Keitel, EPL **94**, 14002 (2011).
[37] B. R. Galloway, D. Popmintchev, E. Pisanty, D. D. Hickstein, M. M. Murnane, H. C. Kapteyn, and T. Popmintchev, Opt. Expr. **24**, 21818 (2016).
[38] E. Pisanty, D. D. Hickstein, B. R. Galloway, C. G. Durfee, H. C. Kapteyn, M. M. Murnane, and M. Ivanov,

arXiv:1606.01931.
[39] A. D. DiChiara, I. Ghebregziabher, R. Sauer, J. Waesche, S. Palaniyappan, B. L. Wen, and B. C. Walker, Phys. Rev. Lett. **101**, 173002 (2008).
[40] N. Ekanayake, S. Luo, P. D. Grugan, W. B. Crosby, A. D. Camilo, C. V. McCowan, R. Scalzi, A. Tramontozzi, L. E. Howard, S. J. Wells, C. Mancuso, T. Stanev, M. F. Decamp, and B. C. Walker, Phys. Rev. Lett. **110** (2013).
[41] C. Hernandez-Garcia, J. A. Perez-Hernandez, T. Popmintchev, M. M. Murnane, H. C. Kapteyn, A. Jaron-Becker, A. Becker, and L. Plaja, Phys. Rev. Lett. **111**, 033002 (2013).
[42] M. Meckel, D. Comtois, D. Zeidler, A. Staudte, D. Pavicic, H. C. Bandulet, H. Pepin, J. C. Kieffer, R. Doerner, D. M. Villeneuve, and P. B. Corkum, Science (N.Y.) **320**, 1478 (2008).
[43] C. I. Blaga, J. Xu, A. D. DiChiara, E. Sistrunk, K. Zhang, P. Agostini, T. A. Miller, L. F. DiMauro, and C. D. Lin, Nature **483**, 194 (2012).
[44] S. Augst, D. Strickland, D. D. Meyerhofer, S. L. Chin, and J. H. Eberly, Phys. Rev. Lett. **63**, 2212 (1989).
[45] L. V. Keldysh, Sov. Phys. JETP **20**, 1307 (1965).
[46] Details are included in the Supplementary Materials.
[47] H. R. Reiss, Phys. Rev. A **42**, 1476 (1990).
[48] M. Klaiber, K. Z. Hatsagortsyan, and C. H. Keitel, Phys. Rev. A **75**, 063413 (2007).
[49] M. Klaiber, E. Yakaboylu, and K. Z. Hatsagortsyan, Phys. Rev. A **87**, 023418 (2013).
[50] V. Popov, V. Mur, and B. Karnakov, JETP Letters **66**, 229 (1997).
[51] V. Mur, B. Karnakov, and V. Popov, JETP Letters **87**, 433 (1998).
[52] N. Milosevic, V. P. Krainov, and T. Brabec, Phys. Rev. Lett. **89**, 193001 (2002).
[53] N. Milosevic, V. P. Krainov, and T. Brabec, J. Phys. B **35**, 3515 (2002).
[54] M. V. Ammosov, N. B. Delone, and V. P. Krainov, Zh. Eksp. Teor. Fiz. **91**, 2008 (1986).
[55] E. A. Chowdhury, C. P. J. Barty, and B. C. Walker, Phys. Rev. A **63**, 042712 (2001).
[56] S. Palaniyappan, A. DiChiara, E. Chowdhury, A. Falkowski, G. Ongadi, E. L. Huskins, and B. C. Walker, Phys. Rev. Lett. **94**, 243003 (2005).
[57] V. S. Popov, Phys. Usp. **47**, 855 (2004).
[58] M. Klaiber, E. Yakaboylu, and K. Z. Hatsagortsyan, Phys. Rev. A **87**, 023417 (2013).
[59] F. Salvat, A. Jablonski, and C. Powell, Computer Physics Communications **165**, 157 (2005).
[60] A. DiChiara, S. Palaniyappan, A. Falkowski, E. Huskins, and B. Walker, J. Phys. B **38**, L183 (2005).
[61] A. D. DiChiara, E. Sistrunk, C. I. Blaga, U. B. Szafruga, P. Agostini, and L. F. DiMauro, Phys. Rev. Lett. **108**, 033002 (2012).
[62] M. Kuebel, C. Burger, N. G. Kling, T. Pischke, L. Beaufore, I. Ben-Itzhak, G. G. Paulus, J. Ullrich, T. Pfeifer, R. Moshammer, M. F. Kling, and B. Bergues, Phys. Rev. A **93**, 053422 (2016).
[63] T. Popmintchev, M. C. Chen, D. Popmintchev, P. Arpin, S. Brown, S. Alisauskas, G. Andriukaitis, T. Balciunas, O. D. Mucke, A. Pugzlys, A. Baltuska, B. Shim, S. E. Schrauth, A. Gaeta, C. Hernández-García, L. Plaja, A. Becker, A. Jaron-Becker, M. M. Murnane, and H. C. Kapteyn, Science **336**, 1287 (2012).